# Asymptotic scattering and duality in the one-dimensional three-state quantum Potts model on a lattice

Ákos Rapp[a], Peter Schmitteckert[b], Gábor Takács[c], Gergely Zaránd[d,e,*]

[a] *Leibniz Universität Hannover, Institut f. Theoretische Physik, Appelstrae 2, 30167 Hannover, Germany*
[b] *Institute of Nanotechnology, Karlsruhe Institute of Technology, 76344 Eggenstein-Leopoldshafen, Germany*
[c] *HAS Theoretical Physics Research Group, Pázmány Péter sétány 1/A, 1117 Budapest, Hungary*
[d] *Freie Universität Berlin, Fachbereich Physik, Arnimallee 14, D-14195 Berlin, Germany*
[e] *BME-MTA Exotic Quantum Phase Group, Institute of Physics, Budapest University of Technology and Economics, H-1521 Budapest, Hungary.*

## Abstract

We determine numerically the single-particle and the two-particle spectrum of the three-state quantum Potts model on a lattice by using the density matrix renormalization group method, and extract information on the asymptotic S-matrix of the quasiparticles. We find that the finite size spectra can be completely understood in terms of a simple effective model introduced in a previous work, and are consistent with an asymptotic S-matrix of an exchange form. The finite size spectra are, on the other hand, inconsistent with a diagonal asymptotic S-matrix, predicted by the bootstrap solution of the corresponding perturbed conformal field theory.

## 1. Introduction

Being the simplest generalization of the transverse field Ising model, the $q$ state quantum Potts model is one of the most paradigmatic models in statistical physics and quantum field theory. The case of $q = 3$ is somewhat peculiar and is of particular interest. In one spatial dimension, the $q = 3$ state quantum Potts model displays a second order quantum phase transition between a ferromagnetic state and a paramagnetic state, just as the transverse field Ising model [1, 2, 3]. The properties of the critical state itself are very well characterized: at the critical point, an exact solution is available [4], and the scaling limit is known to be described in conformal field theory (CFT) by the minimal model of central charge $C = 4/5$ [5, 6], with the so-called $D_4$ partition function in the ADE classification [7]. The ordered and disordered phases of the Potts model are, on the other hand, much richer than those of the transverse field Ising model: Similar to e.g. antiferromagnetic chains of integer spins [8, 9, 10], the gapped phases (i.e., the ferromagnetic as well as the paramagnetic phase)
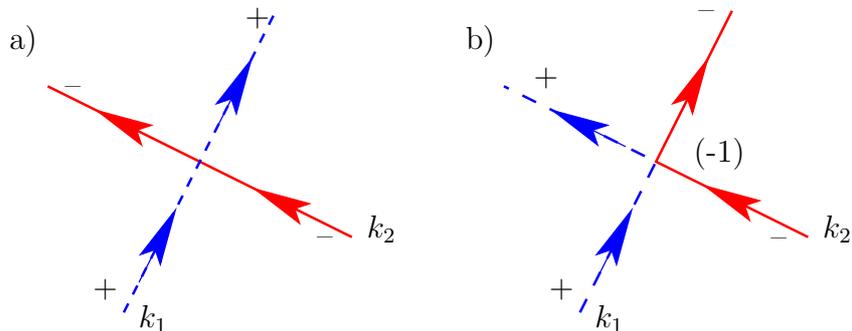
Figure 1: (Color online) Structures of the asymptotic S-matrices. a) Diagonal S-matrix. b) Exchange S-matrix.

possess excitations with internal quantum numbers; as a consequence, the dynamics of these quasiparticles are much richer than those of the transverse field Ising model.

While the critical properties of the Potts model are very well understood, the quasiparticle properties of the gapped phases are somewhat controversial. In the continuum limit, the properties of the Potts model are thought to be described by the so-called scaling Potts field theory, which is a perturbation of the fixed point conformal field theory, uniquely determined by the symmetries. The application of the machinery known as the S-matrix bootstrap [11] yields a diagonal quasiparticle S-matrix for low energy particles [12, 13, 14, 15, 16, 17] and implies that the internal quantum numbers of two colliding particles are conserved during a scattering process (see fig. 1.a) i.e. the scattering process should be pure transmission. The consistency of the bootstrap S-matrix with the perturbed conformal field theory is demonstrated in a separate paper by one of the authors [18].

However, recent calculations on the lattice version of the quantum Potts model contradicted these results [3]: perturbative calculations in both phases as well as rather strong renormalization group arguments yielded a coherent picture, and supported that in the gapped phases, rather than being diagonal, the asymptotic S-matrix of the lattice Potts model assumes the "universal" form emerging in various spin models [9], as well as in the sine-Gordon model [11]: $\hat{S} \to -\hat{X}$, with $\hat{X}$ the exchange operator. According to this result, quasiparticles of small momenta should scatter on each other by exchanging their quantum numbers (see fig. 1.b). We must emphasize that the structure of the asymptotic S-matrix has important physical consequences: an S-matrix of the exchange form yields universal diffusive finite temperature spin-spin correlation functions at intermediate times [3, 19, 20], while a diagonal S-matrix would result in exponentially damped correlations [10, 21, 22].

Although the arguments of Ref. [3] are very robust, the results of Ref. [3] were met by some skepticism. We therefore decided to study in detail the two-particle spectrum of the $q = 3$ state quantum Potts model on a lattice using the powerful numerical method of density matrix renormalization group (DMRG). With this method we are able to compute the finite size spectrum very accurately, and compare it to the predictions of the simple effective theory of Ref. [3], and to those of the bootstrap. As we shall see, the finite size spectra are

in complete agreement with the theory of Ref. [3] and an asymptotic S-matrix of the exchange form, while they obviously disagree with the predictions of the bootstrap, and therefore exclude the corresponding diagonal S-matrix. As we discuss later, we believe that this discrepancy between the continuum approach and the lattice calculations can be traced back to the (incorrect) assumption of integrability, and the presence of "dangerously irrelevant" operators.

## 2. The Potts model and its quasiparticles

In its lattice version, the Potts model consists of a chain of generalized spins having internal quantum states $|\mu\rangle_i$, with $i$ labeling the lattice sites and $\mu = 1, \ldots, q$ the possible internal states of the spins. The Hamiltonian of the $q$-state quantum Potts model is then defined as

$$H = -J \sum_i \sum_{\mu=1}^q P_i^\mu P_{i+1}^\mu - Jg \sum_i P_i \,. \tag{1}$$

Here the traceless operators $P_i^\mu = |\mu\rangle_{ii}\langle\mu| - 1/q$ tend to project the spin at site $i$ along the "direction" $\mu$, and thus the first term of eq. (1) promotes a ferromagnetic ground state, with all spins spontaneously polarized in one of the directions, $|\mu\rangle$. In contrast, the second term in eq. (1) represents a "transverse field", with the traceless operator $P_i = |\lambda_0\rangle_{ii}\langle\lambda_0| - 1/q$ trying to align the spins along the direction $|\lambda_0\rangle \equiv \sum_\mu |\mu\rangle/\sqrt{q}$. The relative strength of these two terms is regulated by the dimensionless coupling, $g$. These terms obviously compete with each other, and their competition leads to a phase transition: for large values of $g$ one finds a paramagnetic phase with a unique ground state, while for small $g$ a ferromagnetic phase appears with $q$ degenerate ground states, spontaneously breaking the global $\mathbb{S}_q$ symmetry. In the $q = 3$ case,— on which we focus here,— the transition occurs at a coupling $g = g_c = 1$, and it is of second order: quasiparticles are gapped on both sides of the transition, but the quasiparticle gap $\Delta$ vanishes continuously at the transition as $\Delta \sim J |g-1|^{5/6}$ [3].

The $q$ state Potts model obviously possesses a global $\mathbb{S}_q$ permutation symmetry. As a consequence, the global cyclic permutation $\mathcal{Z}|\mu\rangle_i = |\mu + 1 \bmod q\rangle_i$ leaves the Hamiltonian also invariant, and can be used to classify its eigenstates as

$$\mathcal{Z}|Q\rangle = e^{i\Omega Q}|Q\rangle, \tag{2}$$

with $Q$ an integer and the angle $\Omega$ defined as $\Omega = 2\pi/q$.[1] In the particular case of $q = 3$, considered here, $Q$ can take values of $Q = 0$ and $Q = \pm$. In this case, pairwise spin exchanges (e.g., $\mu = 1 \leftrightarrow 2$) also imply that states with quantum numbers $Q = \pm$ come in degenerate pairs.

The structure of quasiparticles in the ferromagnetic ($g < 1$) and in the paramagnetic ($g > 1$) phases can be easily understood in the perturbative limits, $g \ll 1$ and $g \gg 1$. For $g > 1$ the ground state $|0\rangle$ is unique, and quasiparticles consist of local spin flips of $\mathbb{S}_3$ charges $Q = \pm$. For $g < 1$, on the other hand, the

---

[1]This holds even in the ferromagnetic phase, but there states with spontaneously broken symmetries must be mixed.

ground state is 3-fold degenerate, $|0) \rightarrow |0)_\mu$, and quasiparticles correspond to domain walls between these ground states, $\mu \rightarrow \mu' = \mu + \theta \mod 3$, with $\theta = \pm$ the quantum number of the domain wall.

Similar to the Ising model, the Potts model is known to be self-dual. High-temperature – low-temperature duality [23] in the $d = 2$ classical Potts model implies a duality $g \leftrightarrow 1/g$ for the quantum Potts model [24]. In the Appendix we show that duality holds even on the level of the matrix elements of the Hamiltonian, and therefore one can map the spectra in the $Q = 0$ sectors for $g$ and $1/g$ by simply rescaling the energies with appropriate factors. We thus have

$$E_n^{Q=0}(g) = g \, E_n^{Q=0}(1/g) \tag{3}$$

for all eigenstates $n$ with periodic boundary conditions (PBC), as also verified later numerically. This duality relation has important consequences, and shall allow us to relate various energy- and length scales on the two sides of the transition.

## 3. Effective theory and two particle S-matrix

In an infinite system, the elementary excitations of the gapped phases can be classified by their momentum, $k$, and for small momenta their energy can be approximated as

$$\epsilon(k) = \Delta + \frac{k^2}{2m} + \dots \tag{4}$$

independently of their internal quantum number. Here $m = m(g)$ is the quasiparticle mass, and $\Delta = \Delta(g)$ denotes the quasiparticle gap.

In the very dilute limit, interactions between quasiparticles can be described in terms of just two-body collisions, and correspondingly, by just two-body scattering matrices and interactions. Assuming pairwise and short ranged interactions between the quasiparticles, one thus arrives at the following effective Hamiltonian (in first quantized form) [3, 10],

$$\mathcal{H} = \sum_{i=1}^{N_{qp}} (\Delta - \frac{1}{2m} \frac{\partial^2}{\partial x_i^2}) + \sum_{i<j} u_{\sigma_i,\sigma_j}^{\sigma_i',\sigma_j'}(x_i - x_j) + \dots \, , \tag{5}$$

with $x_i$ and $\sigma_i$ denoting the coordinates and internal quantum numbers of the quasiparticles, and $N_{qp}$ their number. The above Hamiltonian acts on many-particle wave functions $\psi_{\{\sigma_i\}}(\{x_i\})$, which are bosonic (invariant under exchanges $(x_i, \sigma_i) \leftrightarrow (x_j, \sigma_j)$), and correspond to states of the form $|\psi\rangle = \sum_{\{x_i\}} \sum_{\{\sigma_i\}} \psi_{\{\sigma_i\}}(\{x_i\})|\{x_i\}, \{\sigma_i\}\rangle$. The dots in eq. (5) denote higher order terms, which are irrelevant in the renormalization group sense, and do not influence the asymptotic low-energy properties of the theory.

The scattering of two quasiparticles on each other can be characterized by the two-particle S-matrix, which, in view of the energy and momentum conservation, has a simple structure. The two-particle S-matrix, in particular, relates the amplitude of an incoming asymptotic wave function $\psi_{k_1\sigma_1,k_2\sigma_2}(x_1 \ll x_2) \approx A_{\sigma_1,\sigma_2}^{\text{in}}(k_1, k_2)e^{i(k_1 x_1 + k_2 x_2)}$ with quasiparticle momenta $k_1 > k_2$ to that of the outgoing wave function, $\psi_{k_1\sigma_1,k_2\sigma_2}(x_1 \gg x_2) \approx B_{\sigma_1,\sigma_2}^{\text{out}}(k_1, k_2)e^{i(k_1 x_1 + k_2 x_2)}$ as

$$\mathbf{B}^{\text{out}} = \hat{S}(k_1 - k_2) \, \mathbf{A}^{\text{in}} \, . \tag{6}$$

4

The structure of the two-body S-matrix is further restricted by $\mathbb{S}_3$ symmetry:

$$\hat{S}(k) = \begin{pmatrix} s_3(k) & 0 & 0 & 0 \\ 0 & s_1(k) & s_2(k) & 0 \\ 0 & s_2(k) & s_1(k) & 0 \\ 0 & 0 & 0 & s_3(k) \end{pmatrix}. \tag{7}$$

In the following, we shall only investigate the scattering of quasiparticles in the channels $\{+-\}$ and $\{-+\}$. In these channels, the eigenvalues of the S-matrix read

$$s_t(k) \equiv e^{2i\delta_t(k)} = s_1(k) + s_2(k) , \tag{8}$$
$$s_s(k) \equiv e^{2i\delta_s(k)} = s_1(k) - s_2(k) , \tag{9}$$

where we introduced the "triplet" and "singlet" eigenvalues, $s_t(k)$ and $s_s(k)$, and the corresponding phase shifts, $\delta_t(k)$ and $\delta_s(k)$. As shown in Ref. [3], interactions in the singlet channel are irrelevant for $k \to 0$ (the wave function has a node at $x_1 = x_2$), while they are relevant in the triplet channel, unless some very special conditions are met by the effective interactions [3]. As a result, generically one finds $s_t(k \to 0) = -1$ while $s_s(k \to 0) = 1$, as also confirmed by direct calculations in the $g \to \infty$ and $g \to 0$ limits [3]. As a consequence, by analyticity, the phase shifts must have the following small momentum expansion:

$$\delta_t(k) = -\frac{\pi}{2} \operatorname{sgn}(k) + a_t k + \dots , \qquad \delta_s(k) = -a_s k + \dots . \tag{10}$$

Notice that these expressions (together with $s_3(k \to 0) = -1$) give rise to a low-momentum scattering matrix of the form, $\hat{S} \approx -\hat{X}$. In contrast, perturbed conformal field theory yields a diagonal low-momentum S-matrix with $s_t(k \to 0) = 1$, corresponding to irrelevant interactions even in the triplet channel. However, this would require very special interactions, and is not guaranteed by $\mathbb{S}_3$ symmetry.

### 3.1. Two-particle spectra: paramagnetic phase

The two-particle spectrum of a finite system of size $L \gg a \equiv 1$ follows from the asymptotic form of the S-matrix. In the following, we shall focus exclusively on the simplest case of periodic boundary conditions (PBC).

In the paramagnetic phase, quasiparticles carry a "chirality" label, $\sigma = Q = \pm$. Therefore, the $Q = +$ sector of the spectrum contains single quasiparticle excitations of chirality $\sigma = +$ [described by eq. (4)] as well as, e.g., two-particle excitations with charges $\sigma_1 = \sigma_2 = -$. As a consequence, in the $Q = \pm$ sectors it is numerically hard to separate two-particle states from the single-particle states. We therefore focus on the sector $Q = 0$, where single quasiparticle states are absent, and, above the ground state, the spectrum starts directly with two-particle eigenstates of quasiparticles with charges $\sigma_1 = \pm$ and $\sigma_2 = \mp$.

For large system sizes, the quantization of the momenta $k_1$ and $k_2$ of the quasiparticles is determined by the periodicity condition on the wave function, $\Psi(x_1, x_2) \equiv \Psi(x_1 + L, x_2) \equiv \Psi(x_1, x_2 + L)$, and, just as in Bethe Ansatz, the energy is the sum of the two quasiparticle energies, $E = \epsilon(k_1) + \epsilon(k_2)$. Taking particle $i = 1$ around the system (see fig. 3.1) then yields the following condition,

$$\begin{pmatrix} C_1 \\ C_2 \end{pmatrix} = e^{ik_1 L} \begin{pmatrix} s_1(k_1 - k_2) & s_2(k_1 - k_2) \\ s_2(k_1 - k_2) & s_1(k_1 - k_2) \end{pmatrix} \begin{pmatrix} C_1 \\ C_2 \end{pmatrix} , \tag{11}$$
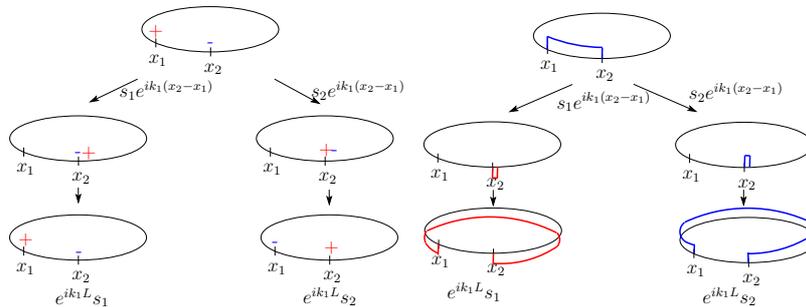
5

Figure 2: (Color online) Translating one of the quasiparticles around by system size $L$ in the paramagnetic (left figure) and ferromagnetic (right figure) phases.

with $C_1 = A_{+-}^{\text{in}}(k_1 \geq k_2)$ and $C_2 = A_{-+}^{\text{in}}(k_1 \geq k_2)$ the wave function amplitudes for $0 < x_1 < x_2 < L$, defined earlier. Taking particle $i = 2$ around, $x_2 \to x_2 + L$, yields a similar equation. In the triplet channel, $C_1 = C_2$, we thus obtain

$$s_t(k_1 - k_2) = e^{-ik_1 L} , \qquad s_t(k_2 - k_1) = e^{-ik_2 L} . \tag{12}$$

Using the asymptotic expansions of the phase shifts, eq. (10), and solving eq. (12) to leading order in $1/L$ then gives

$$E_{n_1,n_2}^t - 2\Delta = \mathcal{E}_0 \left[ \frac{1}{4}(n_1 + n_2)^2 + \frac{1}{4} \frac{(n_1 - n_2 + 1)^2}{(1 + \frac{4a_t}{L})^2} + \mathcal{O}(1/L^2) \right] , \tag{13}$$

where $n_1$ and $n_2$ denote integers, and we introduced the energy unit,

$$\mathcal{E}_0 \equiv \frac{1}{m} \left( \frac{2\pi}{L} \right)^2 . \tag{14}$$

In eq. (13), to comply with the bosonic nature of the excitations, the quantum numbers $n_1$ and $n_2$ must satisfy $n_1 \geq n_2$.

The previous analysis can be carried over to the singlet sector, $C_1 = -C_2$, with little modification, and there it yields the following finite size spectrum:

$$E_{n_1,n_2}^s - 2\Delta = \mathcal{E}_0 \left[ \frac{1}{4}(n_1 + n_2)^2 + \frac{1}{4} \frac{(n_1 - n_2)^2}{(1 - \frac{4a_s}{L})^2} + \mathcal{O}(1/L^2) \right] . \tag{15}$$

However, now $n_1$ and $n_2$ must satisfy $n_1 > n_2$ since for $n_1 = n_2$ the wave function vanishes trivially.

### 3.2. Two particle spectra: ferromagnetic phase

As discussed earlier, the ground state of the infinite system in the ferromagnetic phase has broken $\mathbb{S}_3$ symmetry, and correspondingly, it is 3-fold degenerate, $|0)_\mu$. [2] Excitations are kinks (domain walls), and the corresponding two-particle states read

$$|x_1 \theta_1, x_2 \theta_2)_\mu , \tag{16}$$

---

[2]Here we used brackets rather than angular brackets, to explicitly emphasize that the states $|0)_\mu$ are interacting many-body eigenstates of the Hamiltonian.

with $\mu$ the vacuum polarization at $x \to -\infty$, $x_i$ the positions of the domain steps, and $\theta_i = \pm$ the step sizes. As we shall also demonstrate later through our finite size spectrum analysis, by duality, the S-matrix of these kinks is identical to that of the local spin flip excitations on the paramagnetic side at a corresponding coupling, $g \to 1/g > 1$.

On a ring, PBC implies that $\theta_1 + \theta_2 = 0$. Furthermore, in contrast to the paramagnetic phase, in the ferromagnetic phase one must take into account the presence of the three possible vacuum states when constructing periodic solutions. A way to do that is by keeping track of the vacuum polarization at position $x = 0$, e.g. As a consequence, wave function amplitudes must also have a vacuum label on the ring, $A_{\theta_1 \theta_2} \to A^{(\mu)}_{\theta_1 \theta_2}$. However, there is a subtle difference between scattering in an infinite system and scattering on the ring. As illustrated in fig. 3.1, moving one of the kinks around results not only in a phase change and a collision of the elementary excitations, but the domain orientations also change in a peculiar manner: the configuration essentially turns "inside out". Correspondingly, the amplitudes of the wave functions change as

$$A^{(\mu)}_{+-} \to e^{ik_1 L} s_1(k_1 - k_2)\, A^{(\mu-1)}_{+-} + e^{ik_1 L} s_2(k_1 - k_2)\, A^{(\mu+1)}_{-+} \; . \qquad (17)$$

The states discussed so far are not eigenstates of the cyclic operator, $\mathcal{Z}$ (cf. eq. (2)). However, we can define eigenstates of $\mathcal{Z}$ by taking linear combinations of them. Combining e.g. the three ferromagnetic ground states we find

$$|Q) = \frac{1}{\sqrt{3}} \sum_{\mu} e^{-i\Omega Q \mu} |0)_{\mu} \; . \qquad (18)$$

Similarly, we can define the two particle states, $|x_1\,\theta_1, x_2\,\theta_2; Q)$, and the corresponding scattering states and wave function amplitudes, $A^{Q}_{\theta_1 \theta_2}$, by simply mixing the states and the wave function amplitudes as in eq. (18). Since the quantum number $Q$ is conserved, the periodicity condition of two-particle states simplifies in this basis. Taking the kink $i = 1$ around the ring, the relation in eq. (17) implies the following equation for the amplitudes $C_1 \equiv A^{Q}_{+-}$ and $C_2 \equiv A^{Q}_{-+}$ ,

$$\begin{pmatrix} C_1 \\ C_2 \end{pmatrix} = e^{ik_1 L} \begin{pmatrix} s_1(k_1 - k_2)e^{-i\Omega Q} & s_2(k_1 - k_2)e^{-i\Omega Q} \\ s_2(k_1 - k_2)e^{i\Omega Q} & s_1(k_1 - k_2)e^{i\Omega Q} \end{pmatrix} \begin{pmatrix} C_1 \\ C_2 \end{pmatrix} , \qquad (19)$$

and a similar equation is obtained for moving around particle $i = 2$. The structure of these equations is analogous to those in the paramagnetic case, but the scattering lengths are replaced by some effective $Q$-dependent scattering lengths, $a_{t,s} \to b^{Q}_{t,s}$, yielding the triplet and singlet spectra

$$E^{Q,t}_{n_1,n_2} - 2\,\Delta \;\; = \;\; \mathcal{E}_0 \left[ \frac{1}{4}(n_1 + n_2)^2 + \frac{1}{4} \frac{(n_1 - n_2 + 1)^2}{(1 + \frac{4b^{Q}_t}{L})^2} + \mathcal{O}(1/L^2) \right] ,$$

$$E^{Q,s}_{n_1,n_2} - 2\,\Delta \;\; = \;\; \mathcal{E}_0 \left[ \frac{1}{4}(n_1 + n_2)^2 + \frac{1}{4} \frac{(n_1 - n_2)^2}{(1 - \frac{4b^{Q}_s}{L})^2} + \mathcal{O}(1/L^2) \right] . \qquad (20)$$

Here the lengths $b^{Q}_s$ and $b^{Q}_t$ can be obtained by expanding the phases of the eigenvalues of the matrix in eq. (19),

$$s^{Q}_{s,t}(k) \equiv e^{2i\delta^{Q}_{s,t}(k)} = s_1(k)\cos\Omega Q \mp \sqrt{s_2^2(k) - s_1^2(k)\sin^2 \Omega Q} , \qquad (21)$$

for low momenta. In the $Q = 0$ sector the scattering lengths are thus given by $b_t^{Q=0} = a_t$ and $b_s^{Q=0} = a_s$. The finite size spectrum is thus in agreement with the duality relation, eq. (3), provided that

$$a_t(g) = a_t(1/g) , \qquad a_s(g) = a_s(1/g) .\tag{22}$$

In the $Q = \pm 1$ sector we get, on the other hand,

$$b_t^{Q=\pm 1} = \frac{1}{4}a_t - \frac{3}{4}a_s , b_s^{Q=\pm 1} = \frac{1}{4}a_s - \frac{3}{4}a_t .\tag{23}$$

Equations (20) and (23) are the most important predictions of the effective theory. Together with the duality relation between the ferromagnetic and paramagnetic phases, they allow us to fit the DMRG data on the ferromagnetic side $g < 1$ without any free fitting parameter.

## 4. Numerical results

### 4.1. Technical details

In the numerical calculations, we find the lowest lying eigenstates of the Hamiltonian eq. (1) using the lattice units $J = a = \hbar = 1$. We perform a standard DMRG calculation [25], where we make use of the $\mathbb{S}_3$ symmetry in the Q sector to perform a sub-blocking of the vector space. We use a two site $A \bullet \bullet B$ super block configuration and targeted for up to 15 states lowest in energy. In order to achieve convergence for the larger system sizes, we start with an initial run of targeting the lowest 3 states only, performing 11 finite sweeps and keeping 2000 states per $A/B$ block. We then restart this run increasing the number of low lying target states to 7 and continue with 11, 15 low lying states keeping 2500, 3000, and 4000 states per $A/B$ block performing 5 finite lattice sweeps in each restart. For the 240 site systems we continued restarting the DMRG runs keeping the 15 states lowest in energy and up to $5000 \dots 7000$ states per block. In order to deal with the degeneracies and the large number of low lying states we use the generalized Davidson algorithm ensuring that the solution of the preconditioner $u_n$ is orthogonal to the previously found state $u_{n-1}$ which helps to avoid stagnation of the Davidson algorithm without paying the full overhead of a Jacobi-Davidson scheme. Calculations were performed with a multi threaded code running on eight core machines with 64GB of RAM.

### 4.2. Single-particle levels

The numerically implemented PBC forbids single quasiparticle excitations on the ferromagnetic side, where they can appear only under twisted boundary conditions.[3] In contrast, in the paramagnetic phase the charge of quasiparticles is $Q = \pm$. Therefore, while we could not investigate single quasiparticle excitations in the ferromagnetic phase, we could study them in the paramagnetic phase in the $Q = \pm$ sectors, where they appear as the lowest-lying excitations.

---

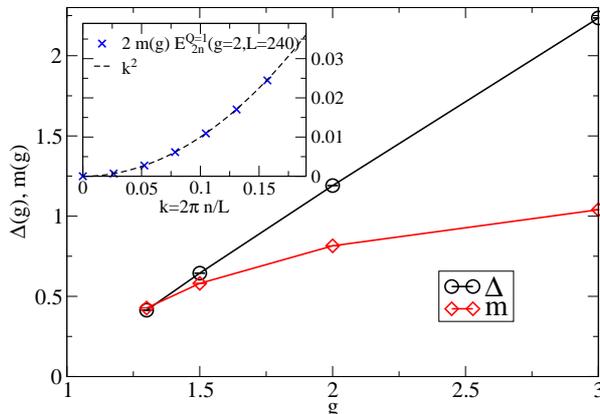[3]Domain wall excitations of the ferromagnetic phase have a $\mathbb{S}_3$ charge $Q = 0$.

Figure 3: (Color online) Single-particle parameters extracted from the DMRG data. Circles denote the quasiparticle gap $\Delta(g)$, while diamonds correspond to the quasiparticle mass $m(g)$. Units of $J = a = \hbar = 1$ are used. The standard error estimated for the fitting is less than the linewidth. Inset: quasiparticle dispersion relation $\epsilon_n - \Delta$ as a function of the momentum $k_n = 2\pi n/L$.

Equation (4) and PBC imply in the $Q = \pm$ sectors of the paramagnetic phase that, for very large systems, the single-particle energies are given by

$$\epsilon_n(g > 1) = \Delta(g) + \frac{1}{2m(g)}\left(\frac{2\pi}{L}n\right)^2 + \dots, \tag{24}$$

with $n \in \mathbb{Z}$. The quasiparticle gap can thus be identified as

$$\Delta(g > 1) \equiv \lim_{L \to \infty}\left(E_{n=0}^{Q=1}(g, L) - E_{n=0}^{Q=0}(g, L)\right), \tag{25}$$

and can be obtained from extrapolating the corresponding numerical data to $L^{-1} \to 0$. The quasiparticle mass $m(g)$ can be defined and extracted through a similar extrapolation procedure.

The single-particle parameters obtained this way are shown in fig. 3. The inset demonstrates that the quadratic dispersion is indeed consistent with the numerically computed excitation spectrum. Both $m$ and $\Delta$ decrease as the coupling approaches the critical value, $g \to 1$, where the gap is supposed to vanish as $\Delta \sim J|g-1|^{5/6}$. The data are consistent with this power-law behavior, but it is difficult to extract the precise value of the critical exponent from them.

The fact that due to the lack of the single-particle excitations, we cannot obtain the quasiparticle parameters on the ferromagnetic side, $g < 1$, directly from the DMRG data is of little concern. The duality relation, eq. (3) relates the quasiparticle gaps and masses in the two phases, since for two remote quasiparticles in a very large system we must have

$$\epsilon(k_1, g) + \epsilon(k_2, g) = g\left(\epsilon(k_1, 1/g) + \epsilon(k_2, 1/g)\right). \tag{26}$$

This can hold for all momenta $k_1, k_2$ only if

$$m(g) = \frac{1}{g}\, m(1/g), \quad \Delta(g) = g\,\Delta(1/g). \tag{27}$$

|     | $\epsilon_{n_1,n_2}$ | $(n_1,n_2)$ | parity | DMRG |
|-----|------|-------------|--------|------|
|     | 1/4 | (0,0) | t | 0.21995 (1×) |
|     | 1/2 | (1,0),(0,-1) | s | 0.50658 (2×) |
| a)  | 1 | (1,-1) | s | 1.02647 (1×) |
|     | 5/4 | (1,0),(0,-1) | t | 1.13124 (2×) |
|     | 5/4 | (1,1),(-1,-1) | t | 1.21941 (2×) |

|     | $\epsilon_{n_1,n_2}^{\mathrm{diag}}$ | $(n_1,n_2)$ | parity |
|-----|------|-------------|--------|
|     | 0 | (0,0) | t |
|     | 1/2 | (1,0),(0,-1) | s |
| b)  | 1/2 | (1,0),(0,-1) | t |
|     | 1 | (1,-1) | s |
|     | 1 | (1,-1) | t |
|     | 1 | (1,1),(-1,-1) | t |

Table 1: a) Asymptotic values of normalized two-particle energies, $\epsilon_{n_1,n_2} \equiv (E_{n_1,n_2} - 2\Delta)/\mathcal{E}_0$, for $L \to \infty$ as predicted by the effective Hamiltonian for a reflective S-matrix in the $Q = 0$ sector of the paramagnetic phase, and the corresponding rescaled energy values, from DMRG (without extrapolation to $L \to \infty$). The DMRG data are taken at $g = 2$ for $L = 240$. b) asymptotic values of energy levels assuming a diagonal S-matrix.

### 4.2.1. Two-particle levels: paramagnetic phase

The prediction of our effective field theory is that for very large system sizes, $L \to \infty$, the excitation spectrum becomes universal in the sense that the rescaled energies, $\epsilon_{n_1,n_2} \equiv (E_{n_1,n_2} - 2\Delta)/\mathcal{E}_0$, approach universal fractions and have corresponding universal degeneracies. Furthermore, eqns. (13),(15) and (20) also predict that corrections to this universal spectrum can be fitted just in terms of two scattering lengths, $a_s$ and $a_t$ for all levels. The predicted universal spectrum, and its comparison with the numerically obtained finite size spectrum is shown in Table 1.a. Already without incorporating finite size corrections, a very good agreement is found: all degeneracies as well as the approximate energies of the states agree very well with the predictions of eqns. (13) and (15). However, as we demonstrate in Table 1.b, the finite size spectrum is completely inconsistent with the spectrum associated with a diagonal S-matrix: there the phase shifts $\delta_{\mathrm{diag}}^s$ and $\delta_{\mathrm{diag}}^t$ vanish for small momenta, and the asymptotic values of the normalized levels are given by $(n_1 + n_2)^2/4 + (n_1 - n_2)^2/4$, with $n_1 \geq n_2$ and $n_1 > n_2$ for the triplet and singlet sectors, respectively. We remark that the same (inconsistent) values are given by the perturbed CFT calculations, discussed in Section 5.

An even more consistent picture based on the effective theory is obtained if one also incorporates $1/L$ corrections due to the finite scattering lengths, $a_s$ and $a_t$. The latter quantities can be extracted from the finite size spectrum by using only the lowest two excited states in the $Q = 0$ subspace

$$a_t(g > 1) \quad = \quad -\lim_{L \to \infty} \frac{L}{2} \left[ \left( E_{n=1}^{Q=0}(g, L) - 2\Delta(g) \right) / \mathcal{E}_0(g, L) - \frac{1}{4} \right], \quad (28)$$

$$a_s(g > 1) \quad = \quad \lim_{L \to \infty} \frac{L}{2} \left[ \left( E_{n=2}^{Q=0}(g, L) - 2\Delta(g) \right) / \mathcal{E}_0(g, L) - \frac{1}{2} \right], \quad (29)$$

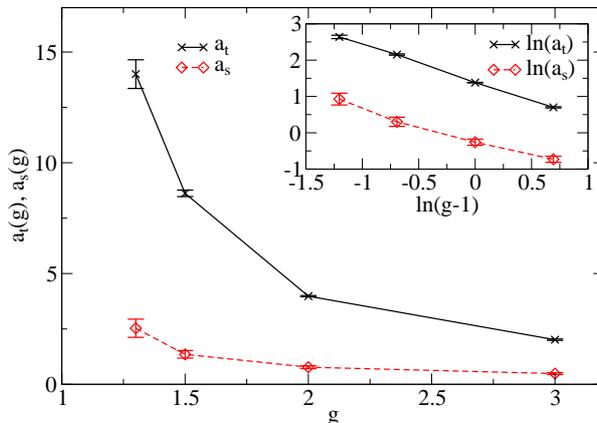respectively. The $g$-dependence of the extracted scattering lengths, $a_s(g)$ and

Figure 4: (Color online) Scattering lengths $a_t(g)$ and $a_s(g)$ as a function of $g$ in units of the lattice constant, $a$. Inset: the logarithms of the scattering lengths as functions of $\ln(g-1)$ show a power law divergence.

$a_t(g)$ is shown in fig. 4. Similar to the correlation length, $a_s$ and $a_t$ both seem to diverge at the critical point, but it is not possible to extract an accurate exponent from our numerical data.

Although the extrapolations in the case of the scattering lengths are less accurate than in the case of the single-particle parameters, we can now plot the higher energy levels in the $Q = 0$ sector using eqns. (13) and (15), and compare them to the appropriately rescaled DMRG data for various system sizes. We find a very good agreement between the numerical results and the predictions for the spectrum of the effective model, as can be seen in fig. 5. A clear convergence to the asymptotic values is observed for large $L$'s, and deviations appear only at smaller system sizes or at higher energy levels, where the asymptotic description must break down.

### 4.2.2. Two-particle levels: ferromagnetic phase

As we discussed before, the spectrum on the ferromagnetic side $g < 1$ with PBC does not have any single-particle levels, from which we could get the quasiparticle parameters directly. Although, in principle, it would be possible to fit the quasiparticle gap and quasiparticle mass along with the scattering lengths from the two-body spectra given by eqns. (20), this is not needed. As discussed earlier, the duality relation, eq. (3) connects energy scales for $g \leftrightarrow 1/g$, and thus $\Delta(g)$ and $m(g)$ through eq. (27) in both phases. In addition, it also implies that all length scales emerging in the problem must be invariant under the duality transformation $g \leftrightarrow 1/g$: relevant length scales appear in the finite size spectrum as cross-over scales, and by the invariance of the spectrum, they must transform similar to the scattering lengths, eq. (22).

Fig. 5 provides an explicit numerical evidence for the duality relation in the $Q = 0$ sector. There we show that the appropriately rescaled DMRG data obtained for $g < 1$ completely overlap with the data on the paramagnetic side $g \to 1/g$. This gives a numerical proof for the relations (3), (22), and (27). We emphasize that the duality relation holds for all system sizes $L$.

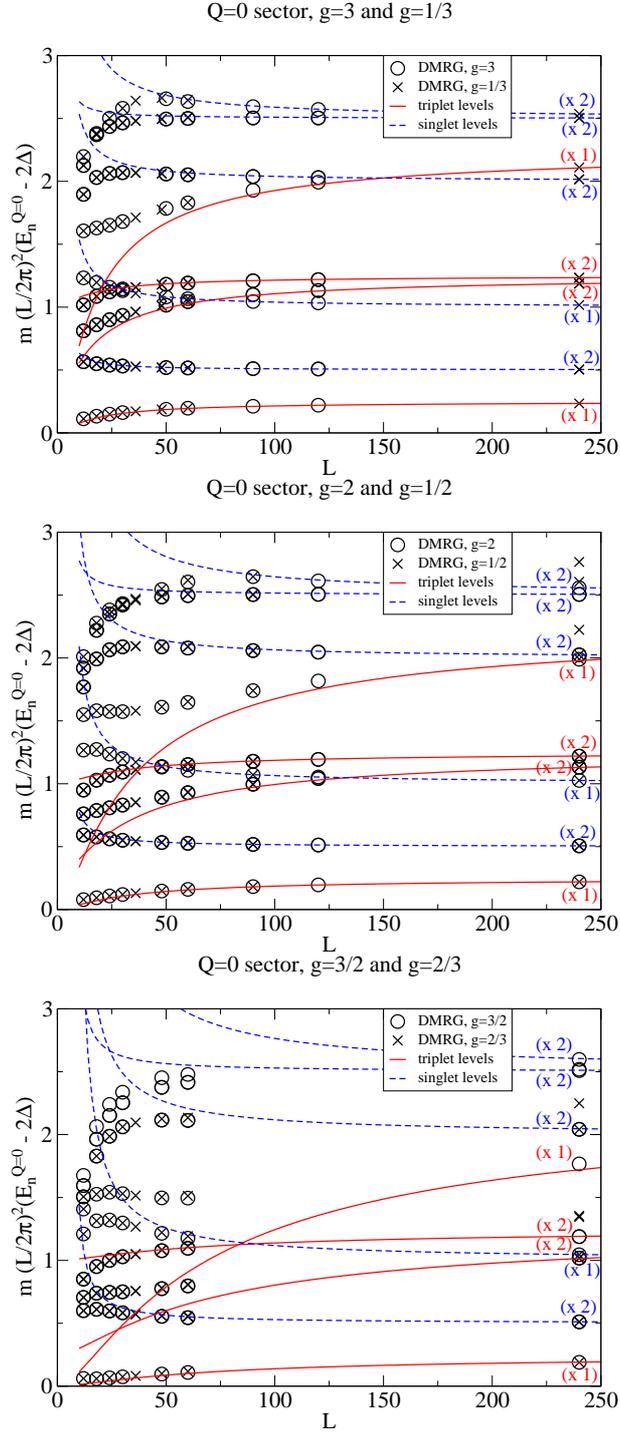In addition to the consistency between the effective theory with a reflective

11

Figure 5: (Color online) Comparison of the rescaled energies from DMRG and the effective theory for $g = 3$, $g = 2$, and $g = 3/2$ in the $Q = 0$ sector. The scattering lengths $a_t$ and $a_s$ were fitted using the lowest lying two levels, respectively. No further fitting for the higher levels was used. Using the duality of the model, we also show the rescaled ferromagnetic spectrum for $\tilde{g} = 1/g$ in the $Q = 0$ sector.

asymptotic S-matrix and the numerical data in the $Q = 0$ sector, probably the most important check of validity of our assumptions is the comparison to the DMRG results in the ferromagnetic $Q = 1$ sector. There the predicted finite size spectrum is given by eqns. (20) together with eq. (23). We emphasize that all parameters of the effective theory are fixed already and no further adjustment to the theoretical spectra is possible. As we show in fig. 6, the effective theory presented here also describes the numerical data in the $Q = 1$ sector within numerical precision in the regime, $\xi \ll L$, and fully confirms eqns. (20) and (23).

## 5. Comparison to the scaling Potts field theory

### 5.1. Scaling Potts field theory as a perturbed conformal field theory

Here we only give a brief review of the scaling Potts field theory; a detailed analysis of the scattering theory is given in a separate paper [18]. The scaling limit of Potts model at the critical point is a minimal conformal field theory with central charge $C = \frac{4}{5}$ [5, 6]. The Kac table of conformal weights is

$$\{h_{r,s}\} = \begin{pmatrix} 0 & \frac{1}{8} & \frac{2}{3} & \frac{13}{8} & 3 \\ \frac{2}{5} & \frac{1}{40} & \frac{1}{15} & \frac{21}{40} & \frac{7}{5} \\ \frac{7}{5} & \frac{21}{40} & \frac{1}{15} & \frac{1}{40} & \frac{2}{5} \\ 3 & \frac{13}{8} & \frac{2}{3} & \frac{1}{8} & 0 \end{pmatrix} \qquad \begin{array}{l} r = 1, \ldots, 4; \\ s = 1, \ldots, 5. \end{array}$$

The sectors of the Hilbert space are products of the irreducible representations of the left and right moving Virasoro algebras which can be specified by giving their left and right conformal weights as

$$\mathcal{S}_{h,\bar{h}} = \mathcal{V}_h \otimes \mathcal{V}_{\bar{h}} \ .$$

There are two possible conformal field theory partition functions for this value of the central charge [7]. The one describing the Potts model is the $D_4$ modular invariant, for which the complete Hilbert space is

$$
\begin{aligned}
\mathcal{H} \ = \ & \mathcal{S}_{0,0} \oplus \mathcal{S}_{\frac{2}{5},\frac{2}{5}} \oplus \mathcal{S}_{\frac{7}{5},\frac{7}{5}} \oplus \mathcal{S}_{3,3} \\
& \oplus \mathcal{S}^+_{\frac{1}{15},\frac{1}{15}} \oplus \mathcal{S}^-_{\frac{1}{15},\frac{1}{15}} \oplus \mathcal{S}^+_{\frac{2}{3},\frac{2}{3}} \oplus \mathcal{S}^-_{\frac{2}{3},\frac{2}{3}} \\
& \oplus \mathcal{S}_{\frac{2}{5},\frac{7}{5}} \oplus \mathcal{S}_{\frac{7}{5},\frac{2}{5}} \oplus \mathcal{S}_{0,3} \oplus \mathcal{S}_{3,0} \ .
\end{aligned}
\tag{30}
$$

Note that not all of the possible representations occur in the Hilbert space; there is another modular invariant partition function called $A_4$ which includes all sectors of diagonal form $\mathcal{S}_{h,h}$ allowed by the Kac table exactly once: $\mathcal{H} = \bigoplus_h \mathcal{V}_h \otimes \mathcal{V}_h$. The $A_4$ model corresponds to the scaling limit of a higher multi-critical Ising class fixed point with symmetry $\mathbb{Z}_2$. In contrast, the $D_4$ conformal field theory is invariant under the permutation group $\mathbb{S}_3$ generated by two elements $\mathcal{Z}$ and $\mathcal{C}$ with the relations

$$\mathcal{Z}^3 = 1 \ , \qquad \mathcal{C}^2 = 1 \ , \qquad \mathcal{C}\mathcal{Z}\mathcal{C} = \mathcal{Z}^{-1} \ ,$$

which have the signatures sign $\mathcal{Z} = +1$ and sign $\mathcal{C} = -1$. The sectors in the first line of (30) are invariant under the action of the permutation group, $\mathbb{S}_3$,
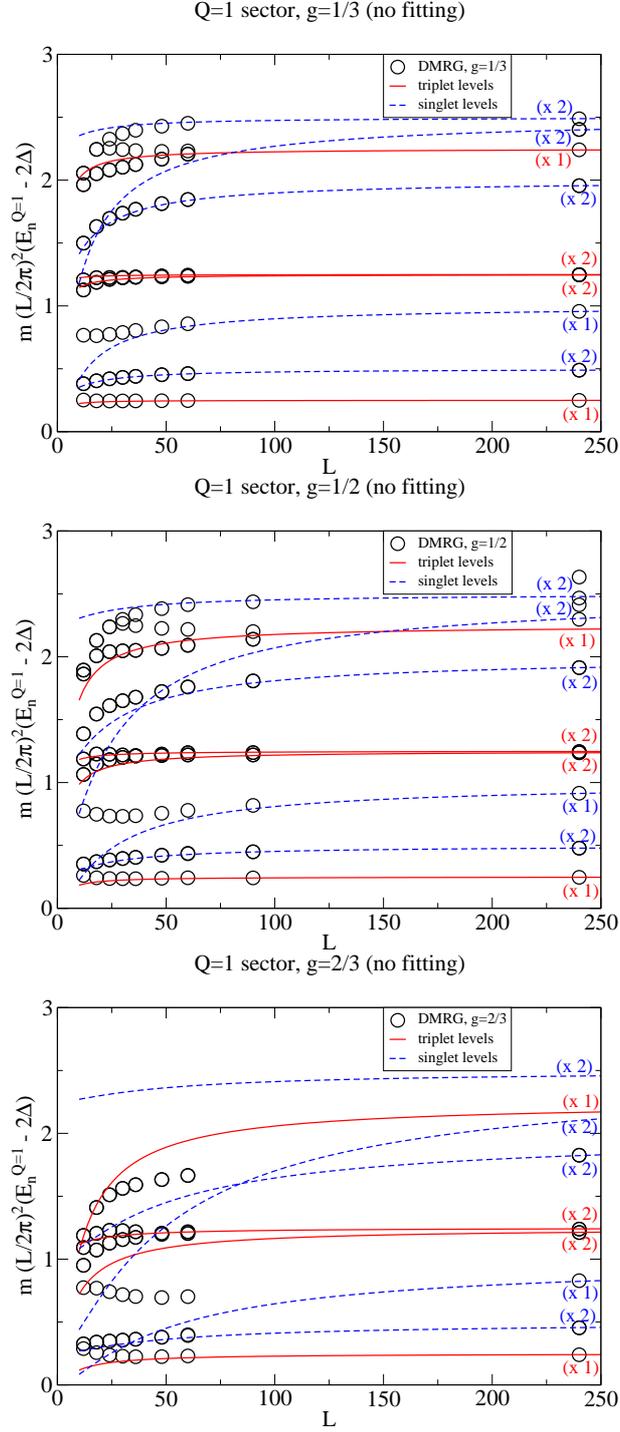
Figure 6: (Color online) The spectra for $g = 1/3$, $g = 1/2$, $g = 2/3$ in the $Q = 1$ sector. Only the numerically converged data points and the corresponding curves from the effective theory are shown.

14

while the two pairs on the second line each form two-dimensional irreducible representations, as characterized by the following action of the generators:

$$\mathcal{C}|\pm\rangle = |\mp\rangle , \quad \mathcal{Z}|\pm\rangle = \mathrm{e}^{\pm i\Omega}|\pm\rangle . \tag{31}$$

Finally, sectors in the third line of eq. (30) form one-dimensional signature representations, where each element is represented by its signature. These sectors are in one-to-one correspondence with the families of conformal fields: the primary field in the family corresponding to $\mathcal{S}_{h,\bar{h}}$ has left and right conformal weights $h$ and $\bar{h}$, and a corresponding scaling dimension, $\Delta_{h,\bar{h}} = h + \bar{h}$, and is denoted by $\Phi_{h,\bar{h}}$, with an optional upper $\pm$ index for fields forming a doublet of $\mathbb{S}_3$.

Relevant fields are exactly those for which $h + \bar{h} < 2$. It is then obvious that the only $\mathbb{Z}_3$-invariant spinless relevant field is $\Phi_{\frac{2}{5},\frac{2}{5}}$, which means that the Hamiltonian of the scaling limit of the off-critical Potts model is uniquely determined [6],

$$H = H_* + \tau \int dx \, \Phi_{\frac{2}{5},\frac{2}{5}} . \tag{32}$$

The sign of the coupling constant $\tau$ corresponds to the two phases: $\tau > 0$ is the paramagnetic, while $\tau < 0$ is the ferromagnetic phase. Up to normalization factor, it is given by

$$\tau \propto (g-1)a^{-6/5} , \tag{33}$$

with $a$ the lattice spacing. The scaling limit is achieved by taking $a \to 0$ and $g \to g_c = 1$ such that $\tau$ remains finite. In this limit, the gap

$$\Delta \sim \tau^{5/6} \sim |g-1|^{5/6} \, \hbar c/a$$

remains also finite. Here, for clarity, we restored $\hbar$ and $c$, which are usually both set to unity in relativistic quantum field theory.

The scaling Potts field theory (32) is known to be integrable [13], and its spectrum and scattering matrix was determined exactly [13, 16]. In the paramagnetic phase, the vacuum is non-degenerate and the spectrum consists of a pair of particles $A$ and $\bar{A}$ of mass $m$, which form a doublet under $\mathbb{Z}_3$ [15]:

$$\begin{aligned}
\mathcal{C}|A(\beta)\rangle &= |\bar{A}(\beta)\rangle , & \mathcal{Z}|A(\beta)\rangle &= \mathrm{e}^{i\Omega}|A(\beta)\rangle , \\
\mathcal{C}|\bar{A}(\beta)\rangle &= |A(\beta)\rangle , & \mathcal{Z}|\bar{A}(\beta)\rangle &= \mathrm{e}^{-i\Omega}|\bar{A}(\beta)\rangle .
\end{aligned} \tag{34}$$

The excitations $A$ and $\bar{A}$ correspond to the local spin flip excitations of chirality $\sigma = Q = \pm$ of the lattice. The generator $\mathcal{C}$ is identical to charge conjugation ($\bar{A}$ is the antiparticle of $A$). Choosing units in which $\hbar = c = 1$, two-dimensional Lorentz invariance implies that the energy and momentum of the particles can be parameterized by the rapidity $\beta$:

$$E = m\cosh\beta , \quad p = m\sinh\beta .$$

The two-particle scattering amplitudes are [13]

$$\begin{aligned}
S_{AA}(\beta_{12}) &= S_{\bar{A}\bar{A}}(\beta_{12}) = \frac{\sinh\left(\frac{\beta_{12}}{2} + \frac{\pi i}{3}\right)}{\sinh\left(\frac{\beta_{12}}{2} - \frac{\pi i}{3}\right)} , \\
S_{A\bar{A}}(\beta_{12}) &= S_{\bar{A}A}(\beta_{12}) = -\frac{\sinh\left(\frac{\beta_{12}}{2} + \frac{\pi i}{6}\right)}{\sinh\left(\frac{\beta_{12}}{2} - \frac{\pi i}{6}\right)} ,
\end{aligned} \tag{35}$$

where $\beta_{12} = \beta_1 - \beta_2$ is the rapidity difference of the incoming particles. This $S$ matrix was confirmed by thermodynamic Bethe Ansatz [26]. We remark that the pole in the $S_{AA} = S_{\bar{A}\bar{A}}$ amplitudes at $\beta_{12} = \frac{2\pi i}{3}$ corresponds to the interpretation of the particle $\bar{A}$ as a bound state of two particles $A$, and similarly, $A$ as a bound state of two $\bar{A}$s, under the bootstrap principle (a.k.a. "nuclear democracy"). The pole in $S_{A\bar{A}} = S_{\bar{A}A}$ amplitudes at $\beta_{12} = \frac{\pi i}{3}$ has a similar interpretation in the crossed channel, and it does not correspond to a true bound state in the neutral sector.

The excitations in the ferromagnetic phase are topologically charged [16]. Similar to the lattice model, the vacuum is three-fold degenerate $|0\rangle_\mu$ ($\mu = -1, 0, 1$). The action of $\mathbb{S}_3$ on the vacua is

$$\mathcal{Z}|0\rangle_\mu = |0\rangle_{\mu+1 \bmod 3} , \qquad \mathcal{C}|0\rangle_\mu = |0\rangle_{-\mu} ,$$

and the excitations are kinks of mass $m$ interpolating between adjacent vacua, and correspond to domain walls on the lattice. The kink of rapidity $\beta$, interpolating from $\mu$ to $\mu'$ is denoted by

$$K_{\mu\mu'}(\beta) , \qquad \mu - \mu' = \pm 1 \bmod 3 .$$

The scattering processes of the kinks are of the form

$$K_{\mu\nu}(\beta_1) + K_{\nu\mu'}(\beta_2) \to K_{\mu\nu'}(\beta_1) + K_{\nu'\mu'}(\beta_2) ,$$

with the scattering amplitudes equal to

$$S\left(\mu \begin{matrix} \nu' \\ \\ \nu \end{matrix} \mu'\right)(\beta_{12}) = \begin{cases} S_{AA}(\beta_{12}) & \text{if} \quad \nu = \nu' , \\ S_{A\bar{A}}(\beta_{12}) & \text{if} \quad \mu = \mu' . \end{cases} \tag{36}$$

This essentially means that, apart from the restriction of kink succession dictated by the vacuum indices (adjacency rules), the following identifications can be made

$$K_{\mu\nu}(\beta) \equiv \begin{cases} A(\beta) & \mu - \nu = +1 \bmod 3 , \\ \bar{A}(\beta) & \mu - \nu = -1 \bmod 3 . \end{cases} \tag{37}$$

in all other relevant physical aspects (such as e.g. the bound state interpretation given above).

The validity of the S-matrix expressions (35) and (36) for the scaling Potts model can be checked by comparing the finite size spectrum of the corresponding Bethe Ansatz equations to that of (32) as obtained by the truncated conformal space approach (TCSA)[4]. This is performed in detail in [18]. In the TCSA, one determines the finite size spectrum of eq. (32) numerically by truncating the finite volume Hilbert space by imposing an upper cutoff in the eigenvalue of the conformal Hamiltonian. For the ground state, this is equivalent to the standard variational calculus in quantum theory, where the variational wave function Ansatz is expressed as a linear combination of a finite subset of the eigenstates of the conformal Hamiltonian. By looking at the conformal fusion

---

[4] The truncated conformal space approach was originally developed in [27].

rules implied by the three-point couplings [28, 29, 30], it turns out that the perturbing operator acts separately in the following four sectors:

$$
\begin{aligned}
\mathcal{H}_0 &= \mathcal{S}_{0,0} \oplus \mathcal{S}_{\frac{2}{5},\frac{2}{5}} \oplus \mathcal{S}_{\frac{7}{5},\frac{7}{5}} \oplus \mathcal{S}_{3,3} \; , \\
\mathcal{H}_\pm &= \mathcal{S}^\pm_{\frac{1}{15},\frac{1}{15}} \oplus \mathcal{S}^\pm_{\frac{2}{3},\frac{2}{3}} \; , \\
\mathcal{H}_1 &= \mathcal{S}_{\frac{2}{5},\frac{7}{5}} \oplus \mathcal{S}_{\frac{7}{5},\frac{2}{5}} \oplus \mathcal{S}_{0,3} \oplus \mathcal{S}_{3,0} \; ,
\end{aligned}
\tag{38}
$$

so the Hamiltonian can be diagonalized separately in each of them. In the lattice language, $\mathcal{H}_\pm$ correspond to the sectors $Q = \pm$, while $\mathcal{H}_0 \oplus \mathcal{H}_1$ span the $Q = 0$ sector. Charge conjugation $\mathcal{C}$ implies that the Hamiltonian is exactly identical in the sectors $\mathcal{H}_+$ and $\mathcal{H}_-$. Furthermore, the spectrum is invariant under transformation, $\tau \to -\tau$ in sectors $\mathcal{H}_0$ and $\mathcal{H}_1$. This is the consequence of a $\mathbb{Z}_2$ symmetry in these sectors, which leaves the fixed point Hamiltonian $H_*$ and the conformal fusion rules in these sectors invariant[5]. Away from the critical point, it can be interpreted as the continuum form of the duality transformation (3) in the scaling limit.

As further discussed in [18], the detailed TCSA calculations indeed confirm that the $S$-matrices (35) and (36) correctly describe the paramagnetic and ferromagnetic phases of the scaling field theory. However, as we discuss below, the Bethe Ansatz spectra computed with (35) and (36) both turn out to be *inconsistent* with the numerically computed finite size spectra.

## 5.2. Comparing the scaling field theory to DMRG

In order to compare the DMRG to the scattering matrices (35,36) directly, we need to rescale the variables to appropriate units in which $c = 1$. The relativistic relation

$$
\Delta = mc^2
$$

allows to determine the speed of light $c = \sqrt{\Delta/m}$ in lattice units $(aJ/\hbar)$. We recall that, according to eq. (4), $\Delta$ is the infinite volume limit of the energy gap between the stationary one-particle state and the ground state, while $m$ can be determined from the large volume behavior of the first excited one-particle state. We then introduce the dimensionless volume variable $(\hbar = 1)$

$$
l = mcL \; ,
$$

i.e. we measure the volume in units of the Compton length. After rescaling the DMRG spectrum to these units, we expect the spectrum of one-particle states to follow the relativistic dispersion,

$$
\begin{aligned}
\frac{1}{\Delta}\left(E(L) - E_0(L)\right) &= \sqrt{1 + \left(\frac{p}{mc}\right)^2} + O\left(e^{-\gamma l}\right) \; , \\
p/mc &= 2\pi \, n/l \; ,
\end{aligned}
$$

where $E_0(L)$ denotes the ground state energy up to exponential finite size corrections. [6] The dispersion above indeed describes the numerically obtained finite

---

[5]The conformal fusion rules do not allow the extension of this symmetry to the $\mathcal{H}_\pm$.

[6]These corrections are due to vacuum polarization and particle self-energy corrections induced by finite volume [31].
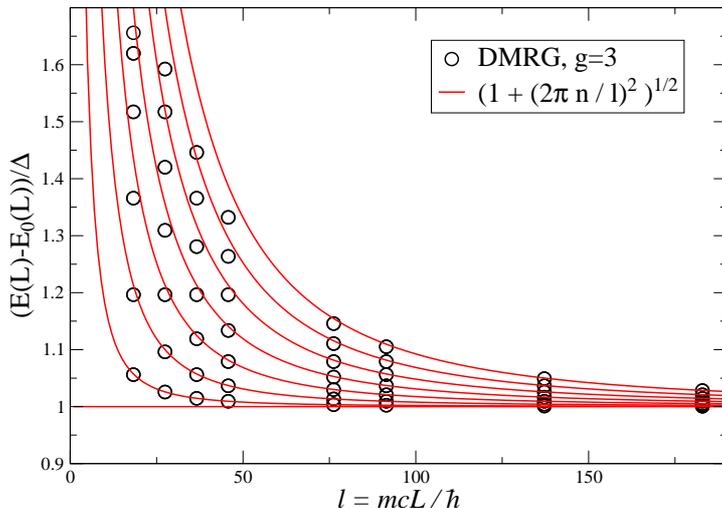
Figure 7: (Color online) Comparing rescaled DMRG data (for $g = 3$) to the relativistic one-particle dispersion relation. Length is measured in the Compton length, $l = mcL/\hbar$.

size spectrum of low energy quasiparticles, as demonstrated in fig. 7. High energy deviations are mainly cut-off effects due to the fact that the DMRG data are not close enough to the fixed point.

Scaling field theory predicts that (neutral) two-particle states in the paramagnetic phase are described by the Bethe-Yang quantization conditions

$$\mathrm{e}^{il\sinh\beta_1}S_{A\bar{A}}(\beta_1 - \beta_2) = 1 , \quad \mathrm{e}^{il\sinh\beta_2}S_{A\bar{A}}(\beta_2 - \beta_1) = 1 ,$$

or, in logarithmic form,

$$
\begin{aligned}
l\sinh\beta_1 + 2\delta_{A\bar{A}}(\beta_1 - \beta_2) &= 2\pi n_1 , \\
l\sinh\beta_2 + 2\delta_{A\bar{A}}(\beta_2 - \beta_1) &= 2\pi n_2 ,
\end{aligned}
$$

with $n_1$ and $n_2$ integer quantum numbers, and the phase-shift function defined as

$$\delta_{A\bar{A}}(\beta) = -\frac{i}{2}\ln S_{A\bar{A}}(\beta) .$$

The Bethe-Yang equations are nothing else than the conditions (11) stated in terms of the notations of the scaling field theory. The energy relative to the ground state can be computed as

$$E(L) - E_0(L) = \Delta\left(\cosh\beta_1 + \cosh\beta_2\right) + O\left(\mathrm{e}^{-\gamma'l}\right) ,$$

and is accurate to all orders in $1/l$, as for the one-particle states. To conform with the conventions used previously, we plot the rescaled quantity

$$\frac{l^2}{(2\pi)^2}\frac{E(L) - 2\Delta - E_0(L)}{\Delta}$$

against $l$. The results are shown in fig. 8, which shows that the scaling field theory correctly describes the singlet levels. In the language of the field theory,
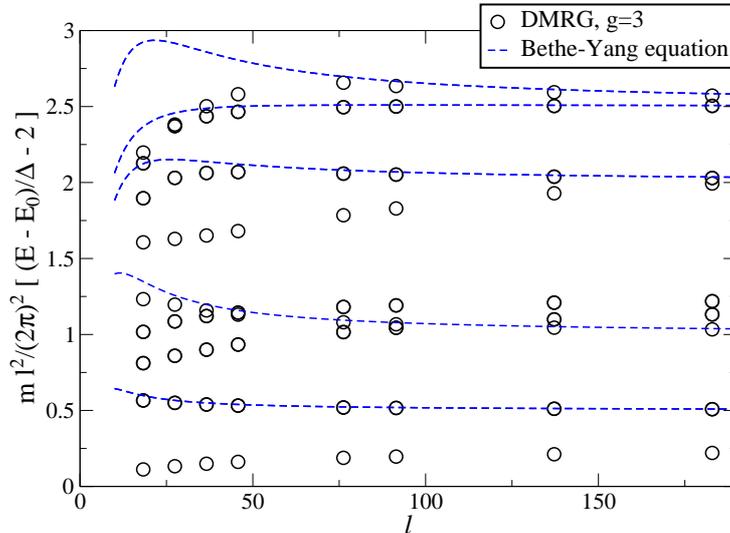
18

Figure 8: (Color online) Comparison of rescaled DMRG data (for $g = 3$) to the two-particle levels predicted by the bootstrap $S$ matrix. While the singlet spectrum is perfectly reproduced without further fitting parameter, the triplet sector cannot be fitted.

these are exactly the two-particle levels in the $\mathcal{C}$-odd sector $\mathcal{H}_1$. However, the triplet levels cannot be explained by the bootstrap $S$ matrix. In the scaling field theory, these levels are in the $\mathcal{C}$-even sector $\mathcal{H}_0$ and are described by the same Bethe-Yang equations, which means that they are exponentially degenerate with their singlet counter-parts. While this picture is fully confirmed by the TCSA analysis [18], it is clearly not consistent with the DMRG spectrum.

To see the problem more clearly, one can perform a direct comparison of the phase-shift function to the DMRG spectrum. Provided the energy levels $E(L)$ are known, the Bethe-Yang equations can be used to extract the phase-shift function from them. The results are shown in fig. 9. For the singlet levels the slope of the phase-shift around the origin agrees quite well with DMRG data, which means that the bootstrap $S$ matrix gives correctly not only the low-energy value of the phase-shift, but also the scattering length. For larger $\beta$ the deviations are explained by cut-off effects since these correspond to lower values of the volume, closer to the scale of the lattice spacing.
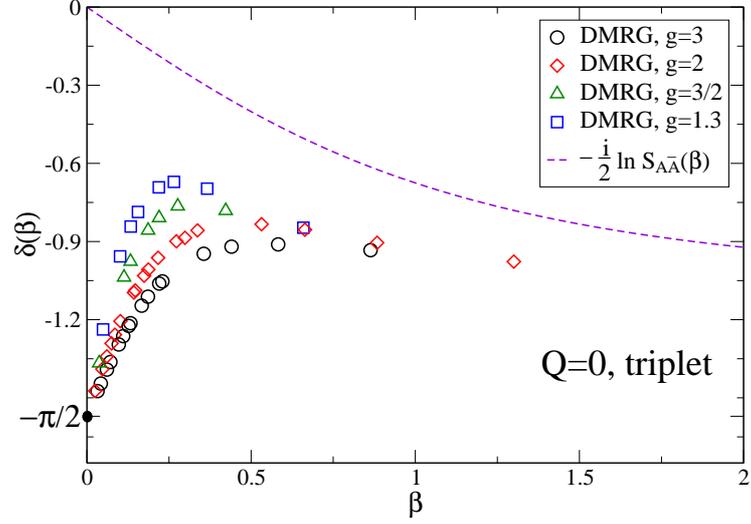
However, the phase-shift extracted from the triplet states does not agree with the bootstrap prediction at all: neither the low-energy value nor the scattering length is consistent as figure 9 (b) demonstrates.

## 6. Conclusions

In this work, we presented an effective low-energy theory to describe the lattice version of the $q = 3$ state quantum Potts model in one dimension. In our approach, the interaction of the quasiparticles is characterized by a scattering matrix, which takes the universal exchange form $\hat{S}(k \to 0) \to -\hat{X}$ in the asymptotic low-momentum limit. A scattering matrix of this form has been first motivated in Ref. [3] by perturbative and renormalization group arguments. To prove (or disprove) the validity of these statements, we calculated the finite
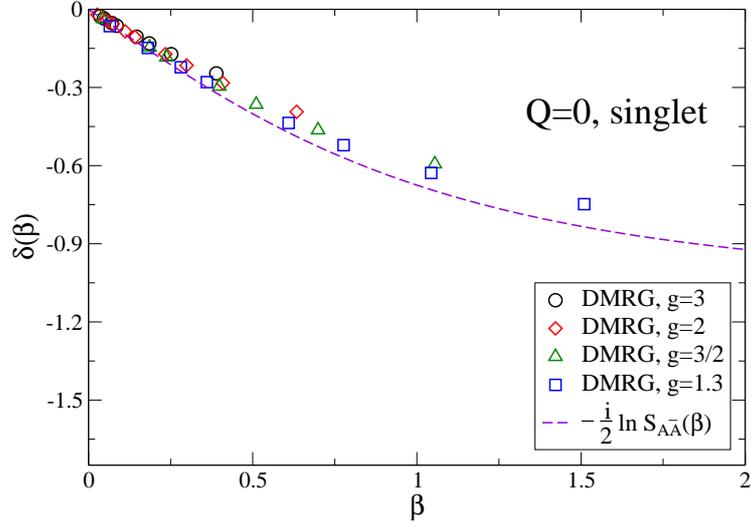
(a)



(b)

Figure 9: (Color online) (a) Singlet phase-shift extracted from DMRG and compared to $\delta_{A\bar{A}}$, as a function of rapidity $\beta$. (b) Triplet phase-shift extracted from DMRG and compared to $\delta_{A\bar{A}}$. Dashed lines are the theoretical predictions from the bootstrap.

size spectra corresponding to this effective theory and compared them to the "numerically exact" energies obtained by density matrix renormalization group calculations as well as to the results from the scaling Potts field theory. The results of this comparison are very clear: the numerically obtained spectrum fully supports the picture of Ref. [3], and it rules out the asymptotic diagonal S-matrix predicted by the scaling Potts field theory. We also find that the bootstrap S matrix is able to reproduce only part of the finite size spectrum (singlet part), and is thus inconsistent with the numerical data.

The structure of the S-matrix can be understood on physical grounds. It is trivial to show that for interacting bosonic quasiparticles in the absence of internal quantum numbers any local interaction is relevant [10], and leads to a scattering phase shift, $\delta = \pm\pi/2$. However, for particles with some nontrivial internal quantum number the situation is somewhat more subtle. In the anti-symmetric (singlet) channel the wave function has a node, and therefore local interactions are asymptotically irrelevant, leading to $\delta_s(k = 0) = 0$. In contrast, in the symmetric (triplet) channel the orbital wave function does not vanish when the two particles approach each other. Here interactions are relevant, and lead to $\delta_t(k = 0) = \pm\pi/2$. These arguments immediately imply an S-matrix of the exchange form. Note that in order to obtain a diagonal S-matrix one needs $\delta_t(k = 0) = 0$. However, this is only possible for very special effective interactions between the quasiparticles [3], and is not guaranteed by $\mathbb{S}_3$ symmetry.

Our numerical calculations also allowed us to check the duality between the ferromagnetic and the paramagnetic states. We have shown that in the $Q = 0$ sector the whole finite size spectrum obeys duality. As a consequence, the scattering lengths, the quasiparticle masses and gaps also satisfy duality relations, as demonstrated by the analysis of the finite size spectra. The extracted scattering lengths seem to diverge at the critical point.

We should also remark that our calculations do not support the existence of bound states in the $\{+-\}$ and $\{-+\}$ channels: every state in the finite size spectrum could be identified as an extended two-particle state. Bound states were also absent in the paramagnetic $Q = \pm$ sectors, where we have just observed extended single particle excitations at and slightly above the gap, $\Delta$, all in agreement with the simple effective theory. We remark that this also agrees with the bootstrap, where particles $A$ and $\bar{A}$ can be interpreted as bound states of $AA$ or $\bar{A}\bar{A}$ in the spirit of Chew's "nuclear democracy"; therefore, one does not expect any additional state besides the multi-particle states built from $A$ and $\bar{A}$ (or the corresponding kinks in the ferromagnetic phase).

Let us finally comment on the discrepancy between the scaling Potts field theory and the properties of the Potts model on a lattice. We believe that the main source of this discrepancy is related to the assumption of *integrability*. Although the $q = 3$ lattice Potts model is integrable at the critical point, $g = 1$, it is believed to be *non*-integrable for other values of $g$. However, the scaling Potts field theory is integrable, and the bootstrap, together with the assumption of $\mathbb{S}_3$ symmetry, leads to a diagonal S-matrix for $q = 3$.[7] Also, in the perturbed CFT description, one perturbs the continuum Potts model with the leading relevant operator, which leaves the model integrable, and gives a spectrum consistent

---

[7]Remarkably, for any other $q \neq 3$ the asymptotic S-matrix assumes the universal exchange form.

with the bootstrap S-matrix (as shown in detail by the analysis in [18]). These methods, at least in their original form, are thus unable to describe the lattice Potts model for $g \neq 1$, probably because requiring integrability conflicts with the true non-integrable nature of the 1+1-dimensional $q = 3$ state lattice Potts model. We think that to describe the $q = 3$ lattice quantum Potts model, one needs to allow for perturbations or cut-off schemes which violate integrability. In perturbed CFT, a possible candidate would be adding the leading irrelevant operator which would violate integrability.

Also, we have to admit that our lattice calculations are still relatively far away from the critical point itself. It is very hard to believe that the asymptotic theory discussed here would suddenly break down as one approaches the critical point, $g = 1$. In this respect, we think that our results are conclusive. However, due to the vanishing of the gap, and the divergence of the correlation length and the scattering lengths, the effective theory will clearly be limited to smaller and smaller momenta, and correspondingly, to smaller and smaller temperature regimes. Indeed, fig. 9.b seems to support the emergence of a new low-energy scale, $\Delta^\star \sim \hbar^2/a_t^2(g)m(g)$, which vanishes faster than $\Delta$ as $g \to g_c$, in agreement with the scenario of irrelevant operators, discussed before. The asymptotic theory is restricted to be valid below this scale, i.e., for quasiparticles of momenta smaller than $\sim 1/a_t$.

Based on the present data we can neither exclude nor admit the possibility that at some intermediate energies a description in terms of the diagonal S-matrix may be adequate. While in the singlet sector, shown in fig. 9 (a), the deviation from the bootstrap solution for intermediate rapidities $\beta \approx 1$ can be explained by the finite UV cutoff, the situation is not so clear in the triplet case, shown in fig. 9 (b). On the one hand, as $g$ approaches the critical point, the phase shift for a small but fixed value of $\beta \neq 0$ seems to slowly approach the curve corresponding to the diagonal S-matrix. On the other hand, while the phase shift seems to have reached the scaling limit for $\beta \approx 1$, the deviation from the bootstrap prediction remains considerably larger than in the singlet case.

## Appendix A. Duality

We show that a one-to-one correspondence (duality relation) exits between the energies in the $Q = 0$ subspace with PBC for couplings $g \leftrightarrow 1/g$. To do this, we introduce two sets of basis states. The first set is defined using the local "spin-flip" states

$$|\{\lambda_i\}\rangle \equiv \prod_{i=1}^{L} |\lambda_i\rangle_i \,, \tag{A.1}$$

where each $\lambda_i \in \{0, 1, -1\}$. Restriction to the $Q = 0$ subspace implies $\sum_{i=1}^{L} \lambda_i = 0$. For a given sequence of $\{\lambda_i\}$, there exists another orthogonal set of dual

states, defined by using the $\lambda_i$ as domain wall labels,

$$|\{\lambda_i\}\rangle \rightarrow |\widetilde{\{\lambda_i\}}\rangle_\mu \equiv \prod_{i=1}^{L} \left| \mu_i = \mu + \sum_{j=1}^{i-1} \lambda_j \right\rangle_i . \tag{A.2}$$

By construction, (since $\sum_{i=1}^{L} \lambda_i = 0$), these states automatically satisfy PBC, but they are not eigenstates of the permutation operator $\hat{C}$. However, we can construct states within the $Q = 0$ subspace by defining

$$\widetilde{|\{\lambda_i\}\rangle} \equiv \frac{1}{\sqrt{3}}[1 + \mathcal{Z} + \mathcal{Z}^2]|\{\lambda_i\}\rangle_{\mu=1}. \tag{A.3}$$

Straightforward algebraic manipulation yields that the matrix elements of the two terms of the Hamiltonian, $H_1 = \sum_i P_i^\mu P_{i+1}^\mu$ and $H_2 = \sum_i P_i$ in eq. (1) satisfy the following identities:

$$\widetilde{\langle\{\lambda_j\}|} \sum_{i,\mu} P_i^\mu P_{i+1}^\mu \widetilde{|\{\lambda'_j\}\rangle} = \langle\{\lambda_j\}| \sum_i P_i |\{\lambda'_j\}\rangle ,$$

$$\widetilde{\langle\{\lambda_j\}|} P_i \widetilde{|\{\lambda'_j\}\rangle} = \langle\{\lambda_j\}| \sum_\mu P_i^\mu P_{i+1}^\mu |\{\lambda'_j\}\rangle. \tag{A.4}$$

Let us now assume that the states

$$|n\rangle = \sum_{\{\lambda_j\}} A_{\{\lambda_j\}}^n |\{\lambda_j\}\rangle \tag{A.5}$$

are normalized, orthogonal eigenstates of $H_1 + gH_2$ in the $Q = 0$ subspace,

$$\langle m|(H_1 + gH_2)|n\rangle = \delta_{nm} E_n(g). \tag{A.6}$$

Then let us define the set of dual states as

$$\widetilde{|n\rangle} \equiv \sum_{\{\lambda_j\}} A_{\{\lambda_j\}}^n \widetilde{|\{\lambda_j\}\rangle}. \tag{A.7}$$

Using eq. (A.4), we immediately see that that these diagonalize the dual Hamiltonian, $H_1 + 1/gH_2$,

$$\widetilde{\langle m|}(H_1 + 1/gH_2)\widetilde{|n\rangle} = (1/g)\langle n|gH_2 + H_1|m\rangle = (1/g)\delta_{nm}E_n(g) , \tag{A.8}$$

yielding the duality relation, eq. (3).

### References

[1] P. Pfeuty, *Ann. Phys.* **57** (1970) 79–90.

[2] F. Y. Wu, *Rev. Mod. Phys.* **54** (1982) 235–268.

[3] Á. Rapp and G. Zaránd, *Phys. Rev.* **B74**, 014433 (2006).

[4] R. Baxter, *Exactly Solved Models in Statistical Mechanics.* Academic Press, 1982.

[5] A. A. Belavin, A. M. Polyakov, and A. B. Zamolodchikov, *Nucl. Phys.* **B241** (1984) 333–380.

[6] V. S. Dotsenko, *Journal of Statistical Physics* **34** (1984) 781–791.

[7] A. Cappelli, C. Itzykson, and J. B. Zuber, *Nucl. Phys.* **B280** (1987) 445–465.

[8] F. D. M. Haldane, *Phys. Lett.* **93A**, 464 (1983).

[9] K. Damle and S. Sachdev, *Phys. Rev.* **B57**, 8307 (1998).

[10] S. Sachdev, *Quantum Phase Transitions* Cambridge University Press, Cambridge, 1999.

[11] A. B. Zamolodchikov and A. B. Zamolodchikov, *Ann. Phys.* **120** (1979) 253–291.

[12] R. Koberle and J. Swieca, *Phys.Lett.* **B86** (1979) 209.

[13] A. B. Zamolodchikov, *Int. J. Mod. Phys.* **A3** (1988) 743–750.

[14] A.M. Tsvelik, *Nucl. Phys.* **B305** (1988) 675–684.

[15] F. A. Smirnov, *Int. J. Mod. Phys.* **A6** (1991) 1407–1428.

[16] L. Chim and A. Zamolodchikov, *Int. J. Mod. Phys.* **A7** (1992) 5317–5335.

[17] P. Fendley and N. Read, J. Phys. A **35**, 10675 (2002).

[18] G. Takács, "Finite volume analysis of the scattering theory in the scaling Potts model", `arXiv:1112.nnnn [cond-mat.stat-mech]`.

[19] K. Damle and S. Sachdev, Phys. Rev. Lett. **95**, 187201 (2005).

[20] Á. Rapp and Gergely Zaránd, *Eur. Phys. J.* **B67** (2009) 7–13.

[21] S. Sachdev and A. P. Young, *Phys. Rev. Lett.* **78** (1997) 2220.

[22] B. L. Altshuler, R. M. Konik, and A. M. Tsvelik, *Nucl. Phys.* **B739** (2006) 311–327.

[23] L. Mittag and M. J. Stephen, *J. Math. Phys.* **12** (1971) 441.

[24] J. Sólyom, *Phys. Rev.* **B24** (1981) 230–243.

[25] S. R. White, Phys. Rev. Lett **69** (1992) 2863; Phys. Rev. B **48**, (1993) 10345.

[26] A. B. Zamolodchikov, *Nucl. Phys.* **B342** (1990) 695–720.

[27] V. P. Yurov and A. B. Zamolodchikov, "Truncated conformal space approach to scaling Lee-Yang model," *Int. J. Mod. Phys.* **A5** (1990) 3221–3246.

[28] J. Fuchs and A. Klemm, *Ann. Phys.* **194** (1989) 303.

[29] V. B. Petkova, *Phys. Lett.* **B225** (1989) 357.

[30] V. B. Petkova and J. B. Zuber, *Nucl. Phys.* **B438** (1995) 347–372.

[31] M. Lüscher, *Commun. Math. Phys.* **104** (1986) 177.